A structural comparison of molybdenum cofactor-containing enzymes

Caroline Kisker [a], Hermann Schindelin [b], Dietmar Baas [c], Janos Rétey [c],
Rainer U. Meckenstock [d], Peter M.H. Kroneck [d],*

[a] *Department of Pharmacological Sciences, School of Medicine, SUNY Stony Brook, Stony Brook, NY 11794-8651, USA*
[b] *Department of Biochemistry and Cell Biology, SUNY Stony Brook, Stony Brook, NY 11794-5215, USA*
[c] *Institut für Organische Chemie, Lehrstuhl Biochemie, Universität Karlsruhe, D-76128 Karlsruhe, Germany*
[d] *Fakultät für Biologie, Universität Konstanz, D-78457 Konstanz, Germany*

Abstract

This work gives an overview of the recent achievements which have contributed to the understanding of the structure and function of molybdenum and tungsten enzymes. Known structures of molybdo-pterin cofactor-containing enzymes will be described briefly and the structural differences between representatives of the same and different families will be analyzed. This comparison will show that the molybdo-pterin cofactor-containing enzymes represent a very heterogeneous group with differences in overall enzyme structure, cofactor composition and stoichiometry, as well as differences in the immediate molybdenum environment. Two recently discovered molybdo-pterin cofactor-containing enzymes will be described with regard to molecular and EPR spectroscopic properties, pyrogallol-phloroglucinol transhydroxylase from *Pelobacter acidigallici* and acetylene hydratase from *Pelobacter acetylenicus*. On the basis of its amino acid sequence, transhydroxylase can be classified as a member of the dimethylsulfoxide reductase family, whereas classification of the tungsten/molybdenum-containing acetylene hydratase has to await the determination of its amino acid sequence. © 1999 Published by Elsevier Science B.V. All rights reserved.

Keywords: Molybdo-pterin; Transhydroxylase; Molybdenum enzymes; Tungsten enzymes; Iron–sulfur cluster; Acetylene hydratase

Contents

* Corresponding author. Tel.: +49 (7531) 882103; Fax: +49 (7531) 882966; E-mail: peter.kroneck@uni-konstanz.de

1. Introduction

The molybdenum cofactor (Mo-co) is found in a variety of enzymes called hydroxylases or oxotransferases, most of which catalyze a net transfer of an oxygen atom to or from a substrate in a two electron transfer reaction [1–4]. An essential role of molybdenum is the catalysis of a controlled oxo-transfer reaction coupled to an electron transfer between substrates and other cofactors, such as Fe–S centers, hemes, and flavins. Molybdenum oxotransferase enzymes, such as xanthine oxidase, catalyze the following general reactions, where water has been shown to be the source of the incorporated oxygen atom:

$$RH + H_2O^* \rightarrow RO^*H + 2e^- + 2H^+$$

(RH = aldehyde or aromatic heterocycle).

Sulfite oxidase catalyzes a simple oxotransfer to the lone pair of sulfite to form sulfate. In a similar type of reaction DMSO reductase transforms dimethylsulfoxide into dimethylsulfide, whereas in nitrate reductase, the reverse reaction occurs and nitrite is produced from nitrate.

The Mo-co consists of an organic component called molybdopterin [5,6], a substituted pterin derivative containing a 4-carbon side chain with a dithiolene group (Fig. 1), and a mononuclear molybdenum or tungsten center. The cofactor was initially believed to occur only in a molybdenum-containing form, hence the names molybdopterin and Mo-co, but recently a tungsten-containing form of the cofactor was also discovered [7,8]. In either case, the metal is ligated to the molybdopterin through the sulfur atoms of the dithiolene group. The first crystal structure of an enzyme containing a molybdopterin cofactor was that of the tungstoenzyme aldehyde ferredoxin oxidoreductase (AOR) from the hyperthermophilic organism *Pyrococcus furiosus* [9]. Subsequently, several structures of 'true' Mo-co-containing enzymes were determined by X-ray crystallography, aldehyde oxidoreductase from *Desulfovibrio gigas* [10,11], dimethylsulfoxide (DMSO) reductase from *Rhodobacter sphaeroides* [12] and *Rhodobacter capsulatus*, independently studied by two groups [13,14], *Escherichia coli* formate dehydrogenase H [15] and, most recently, chicken sulfite oxidase [16].
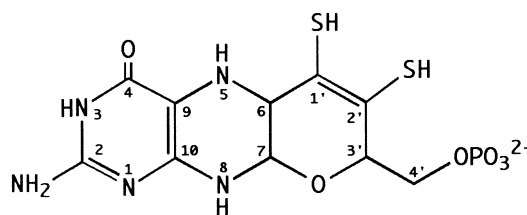

Fig. 1. Structure of the organic component of the molybdenum cofactor (Mo-co) in the tricyclic form as observed in all crystal structures of enzymes containing this cofactor. The atom-numbering scheme used in the text is indicated.

Based on sequence similarities, the Mo-co-containing enzymes are currently divided into four different families [17], namely the DMSO reductase, xanthine oxidase, sulfite oxidase, and AOR families. Within each family, sequence similarities are obvious, while no significant homologies can be detected between members of different families. This classification represents a unifying approach in terms of the overall enzyme structure, but, at the same time, it does not require the Mo/W center to be coordinated in exactly the same way for members of the same family. The traditional classification of these enzymes into two families, one containing an oxothio Mo center and the other containing a dioxo Mo center was based solely on the molybdenum environment and, with the knowledge of the crystal structures, proved to be inadequate for a general classification of these enzymes. The features of the new classification scheme are illustrated best by DMSO reductase and formate dehydrogenase H, two members of the DMSO reductase family. These enzymes share a significant overall structural similarity, which is a consequence of their 23% identical amino acid sequence, but they differ in terms of their respective Mo-ligand fields: DMSO reductase has at least one oxo-ligand and a serine side chain coordinated to the Mo, whereas formate dehydrogenase H contains no oxo-ligand and a seleno-cysteine side chain ligated to the metal. With the exception of *Rhodobacter* DMSO reductase, all enzymes contain at least one additional cofactor, either a heme, a Fe–S cluster, or a flavin, which is involved in intramolecular electron transfer to or from the Mo/W center.

In this contribution, the known structures of Mo-co-containing enzymes will be described briefly and the structural differences between representatives of the same and different families will be analyzed. This comparison will show that the Mo-co-containing enzymes represent a very heterogeneous group with differences in overall enzyme structure, cofactor composition and stoichiometry, as well as differences in the immediate molybdenum environment. Two recently discovered Mo-co-containing enzymes will be described in more detail, pyrogallol-phloroglucinol transhydroxylase from *P. acidigallici* and acetylene hydratase from *P. acetylenicus*. On the basis of the transhydroxylase amino acid sequence, this enzyme can be classified as a member of the DMSO

Table 1
Mo-co-containing enzyme families and selected representatives

DMSO reductase family	
DMSO reductase	*Rhodobacter sphaeroides*, *Rhodobacter capsulatus*, *Escherichia coli*
Nitrate reductase (dissimilatory)	*Escherichia coli* (*narGHI*), *Escherichia coli* (*narZYW*)
Formate dehydrogenase	*Escherichia coli* (*fdnGHI*), *Escherichia coli* (*fdoGHI*)
Pyrogallol-phloroglucinol transhydroxylase	*Pelobacter acidigallici*
Xanthine oxidase family	
Xanthine oxidase/dehydrogenase	*Bos taurus*, *Homo sapiens*, *Gallus gallus*
Aldehyde oxidoreductase	*Desulfovibrio gigas*
Sulfite oxidase family	
Sulfite oxidase	*Homo sapiens*, *Rattus norvegicus*, *Gallus gallus*, *Thiobacillus novellis*
Nitrate reductase (assimilatory)	*Neurospora crassa*, *Chlorella vulgaris*, *Spinacea oleracea*
Aldehyde ferredoxin oxidoreductase family	
Aldehyde ferredoxin oxidoreductase	*Pyrococcus furiosus*
Formaldehyde ferredoxin oxidoreductase	*Pyrococcus furiosus*
Glyceraldehyde-3-phosphate ferredoxin oxidoreductase	*Pyrococcus furiosus*
Carboxylic acid reductase	*Clostridium formicoaceticum*
Aldehyde dehydrogenase	*Desulfovibrio gigas*
Unclassified at present	
Acetylene hydratase	*Pelobacter acetylenicus*

reductase family, whereas classification of the tungsten-containing acetylene hydratase has to await the determination of its amino acid sequence.

2. DMSO reductase family

Members of this family are exclusively found in eubacteria and include among others DMSO reductase, the dissimilatory nitrate reductases, several formate dehydrogenases and pyrogallol-phloroglucinol transhydroxylase (Table 1). With the exception of transhydroxylase, most of these enzymes serve as terminal reductases in the absence of oxygen and the presence of their respective substrates, thereby allowing the bacteria to generate more energy compared to the amount obtainable by fermentation. DMSO reductase is found in a variety of bacteria, including *E. coli* [18], *R. sphaeroides* [19] and *R. capsulatus* [20]. DMSO reductase from *R. sphaeroides* is a soluble periplasmic single subunit protein comprising 780 residues which contains no cofactor other than Mo-co. In contrast, the *E. coli* enzyme is an integral membrane protein consisting of three subunits: (1) the Mo-co-containing A-subunit; (2) a B-subunit with four [4Fe–4S] clusters; and (3) a transmembrane C-subunit also responsible for binding and oxidation of menaquinol. Electrons are transferred from the C-subunit, via the B-subunit to the Mo-co. A more complex architecture is also observed for the cytosolic pyrogallol-phloroglucinol transhydroxylase which consists of a Mo-co-containing A-subunit and a Fe–S cluster containing B-subunit. At present, two members of the DMSO reductase family have been characterized structurally by X-ray crystallography: DMSO reductase, both from *R. sphaeroides* [12] and *R. capsulatus* [13,14], and *E. coli* formate dehydrogenase H [15].

2.1. Structure of DMSO reductase

The crystal structure of the single subunit DMSO reductase from *R. sphaeroides* was determined in its oxidized and dithionite reduced state [12] and the *R. capsulatus* enzyme was determined in its oxidized [13,14], in the dithionite reduced state [13] and in complex with DMSO [21]. The enzyme from *R. sphaeroides* is a mixed α/β-protein and the polypeptide fold consists of four domains arranged around the cofactor, which, in this case, is comprised of two molecules of a molybdopterin guanine dinucleotide. The four domains form a slightly elongated molecule (Fig. 2) with overall main chain dimensions of $75 \times 55 \times 65$ Å^3. The spatial arrangement of domains I–III creates a large depression on one side of the molecule resembling a funnel, with the active site located at the bottom of the funnel. Domain I is formed by two three-stranded antiparallel β-sheets and three α-helices and is the only domain that forms no direct interactions with the cofactor. Domain II has an α/β-fold, containing a mixed six-stranded β-sheet and nine α-helices distributed on either side of the sheet. One of the β-strands is antiparallel to the other five strands. The third domain is located on the opposite side of the cofactor relative to the second domain and is also of the α/β-type, with a strictly parallel five stranded β-sheet surrounded by 12 α-helices. The fold of domain III is a variant of the classical dinucleotide binding domain [25], containing five instead of six parallel β-strands. Domain IV is located between the second and third domain on the opposite side of the funnel, and consists mainly of a six-stranded β-barrel, containing both antiparallel and parallel strands. Domain IV has the same fold as 'barwin' [26] and endoglucanase V from *Humicola insolens* [27]. Structure-based sequence alignments of the DMSO reductase family of Mo-co-containing enzymes demonstrate that conserved regions are mainly located in the core of domains II and III, as well as in the entire domain IV, indicating that these enzymes all share the same basic architecture.

Although the electron density was well defined for almost all parts of the polypeptide chain, a polypeptide loop comprising residues 381–393 was found to be disordered in all crystal structures of the oxidized enzyme. In *R. sphaeroides* DMSO reductase, residual density near the active site was assigned to the side chain of Trp-388 in two alternate conformations. In one of them, Trp-388 blocks access to the active site by insertion of its side chain between the aromatic ring systems of Tyr-165 and Trp-196. In the other conformation, the side chain is displaced by approximately 7 Å and is arranged perpendicular to that of Trp-196. These observations suggested that Trp-388 might serve as a lid that can shield the active site
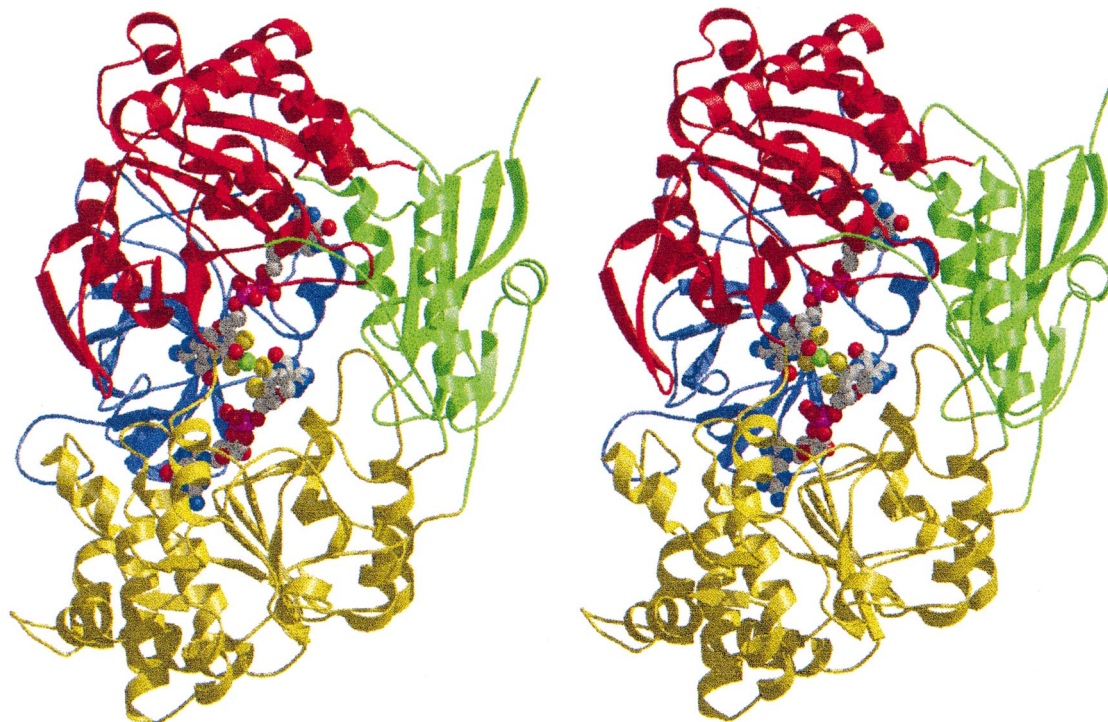
Fig. 2. Overall structure of *R. sphaeroides* DMSO reductase. Schematic ribbons stereo drawing viewed into the active site funnel with domain I in green, domain II in yellow, domain III in red and domain IV in blue. The cofactor is shown in a space filling representation. Atoms are color-coded with molybdenum in green, sulfur in yellow, oxygen in red, nitrogen in blue and carbon in grey. Fig. 2 and Figs. 4–6, have been prepared using MOLSCRIPT [22] and RASTER3D [23,24].

when necessary. In the structure of DMSO reductase from *R. capsulatus* in complex with DMSO [21], the flexible polypeptide loop was found to be ordered and to participate in interactions with the substrate.

2.2. Active site structure

The active site of DMSO reductase in both *R. sphaeroides* and *R. capsulatus* was found to contain two molybdopterin guanine dinucleotides, named P- and Q-pterin, which coordinate the Mo with an approximate two-fold axis of symmetry passing through the Mo. The active site of the enzyme is located at the bottom of the large depression in the protein described above. The two halves of the cofactor are arranged in an antiparallel fashion and form an elongated structure with a maximum extent of ~ 35 Å between the N2 atoms of the two guanine moieties. There are numerous interactions between the protein and the cofactor in addition to a few

hydrogen bonds to water molecules, which are not located in the vicinity of the Mo atom. Residues interacting with the cofactor are scattered throughout the linear sequence and are located in domains II, III, and IV. Domains II and III interact primarily with each of the guanosines and share structural similarity despite the lack of sequence homology. A stretch of highly conserved residues forming a polypeptide loop in domain IV is crucial for binding of the two molybdopterin moieties of the cofactor. Sequence comparisons reveal that several cofactor ligands are highly conserved in the DMSO reductase family.

The coordination features of the Mo in the existing DMSO reductase crystal structures and the models derived by EXAFS spectroscopy are summarized in Table 2. It is apparent that there is considerable disagreement in the nature and distances of some of the molybdenum ligands. A superposition of the three crystal structures indicates rather large shifts

in the position of the molybdenum, with a maximum difference of 1.2 Å between the two structures of the *R. capsulatus* enzyme. As a result of this shift, the molybdenum is either coordinated by both or by none of the dithiolene sulfurs from the Q-pterin in the *R. capsulatus* enzyme. In *R. sphaeroides* DMSO reductase, an intermediate state is observed with one of the sulfurs being partially removed from the Mo. In the coordination models derived by EXAFS spectroscopy, all four dithiolene sulfurs are ligands to the molybdenum. In the *R. capsulatus* model, two sulfurs are at 2.32 Å and two are at 2.47 Å, whereas they are equidistant in the *R. sphaeroides* model. The existence of a second non-protein oxygen ligand is an additional feature of the molybdenum coordination that is at variance. In the crystal structure and EXAFS model of the *R. sphaeroides* enzyme this oxygen is absent, whereas it has been observed in all models derived for the *R. capsulatus* enzyme. However, whether this ligand is an oxo-species or a hydroxo remains unclear. The EXAFS data and one crystal structure indicate a longer distance for the second oxygen, whereas the two non-protein oxygens are equidistant from the Mo in the second crystal structure. EPR studies of the *R. capsulatus* enzyme have identified at least five different signals [30], indicating considerable flexibility at the active site. Furthermore, as has been discussed recently [31], the metal ligand distances derived in typical protein crystal structures at less than atomic resolution are influenced by series termination errors in the Fourier calculations, and therefore it might be difficult to distinguish between oxo- or hydroxo-ligands. At present, the reasons for the observed structural differences at the active site of DMSO reductase are not fully understood and future studies are necessary to address this issue.

2.3. Formate dehydrogenase H from E. coli

The crystal structure of *E. coli* formate dehydrogenase H [15] has confirmed several structural features for all members of the DMSO reductase family. These include the overall architecture of the enzyme, which also was found to consist of four domains, the presence of two molybdopterin guanine dinucleotides and a protein side chain ligand to the Mo, in this case a Se-cysteine. The coordination sphere of the Mo is comprised by four sulfurs originating from the two dithiolene groups, symmetrically coordinating the Mo, by a selenium from the Se-cysteine and by a hydroxyl species. Thus, the coordination sphere of the molybdenum is devoid of any oxo-ligand. The basic features of this coordination geometry have been confirmed by EXAFS spectroscopy, with the addition of a rather short distance between the selenium and one of the dithiolene sulfurs which has been interpreted as a Se–S bond [32]. The additional cofactor of this enzyme, a [4Fe–4S] cluster is located in the N-terminal domain in close proximity to the Mo-co and this arrangement has implicated the Q-pterin to participate in the electron transfer reaction. Large conformational changes for the molybdopterin moiety of the P-pterin were observed between the Mo(IV) and Mo(VI) forms of the enzyme. Binding of the inhibitor NO_2^- suggested direct substrate binding to the Mo and a hydride transfer mechanism involving the Se-cysteine has been suggested [15,33].

Table 2
Molybdenum-ligand distances in *R. sphaeroides* and *R. capsulatus* DMSO reductase as determined by X-ray crystallography and EXAFS spectroscopy for the oxidized form of the enzyme

	R. sphaeroides X-ray [12]	*R. capsulatus* X-ray (1) [14]	*R. capsulatus* X-ray (2) [13]	*R. sphaeroides* EXAFS [28]	*R. capsulatus* EXAFS [29]
Ligands	5–6	5	7	6	7
Mo-S1″ P (Å)	2.4	2.5	2.4	2.44	2.32 or 2.47
Mo-S2″ P (Å)	2.4	2.43	2.5	2.44	2.32 or 2.47
Mo-S1″ Q (Å)	2.4	not a ligand	2.4	2.44	2.32 or 2.47
Mo-S2″ Q (Å)	3.1	not a ligand	2.5	2.44	2.32 or 2.47
Mo-Oγ S147 (Å)	1.7	1.9	1.9	1.92	1.92 or 2.27
Mo-O1 (Å)	1.7	1.7	1.6	1.68	1.71
Mo-O2 (Å)	not present	1.7	1.8	not present	1.92 or 2.27

3. Pyrogallol-phloroglucinol transhydroxylase from *P. acidigallici*

3.1. Molecular properties and reactivity

Transhydroxylase from the anaerobic bacterium *P. acidigallici* catalyzes the conversion of pyrogallol (1,2,3-trihydroxybenzene) to phloroglucinol (1,3,5-trihydroxybenzene) which is further degraded to acetate via the phloroglucinol pathway [34]. 1,2,3,5-Tetrahydroxybenzene is used as a co-substrate and regenerated in the reaction [35]. For a discussion of this novel type of reaction refer to the contribution by Hille et al. in this volume.

The enzyme is a 133.3-kDa heterodimer, composed of one 100.4- and one 31.3-kDa subunit. It contains 11.56 ± 1.72 Fe and 0.96 ± 0.21 Mo (atomic absorption spectroscopy), and 13.13 ± 1.68 acid labile sulfur per heterodimer. Furthermore, one molybdopterin guanine dinucleotide per subunit had been postulated [36,37]. The enzyme has been crystallized and the solution of the structure is in progress.

3.2. Sequence analysis and expression of the transhydroxylase genes

Sequencing showed that the transhydroxylase from *P. acidigallici* belongs to the family of the DMSO reductases (Table 3). In all members of this family, the coenzyme is a dimeric molybdopterin guanine dinucleotide. In Table 4, the contacts of the cofactor to amino acid residues of DMSO reductase of *Rhodobacter sphaeroides* [12] are shown together with the correlating amino acids in transhydroxylase as examined by the program GAP [49]. Although not all of these amino acids are conserved in the molybdopterin guanosine dinucleotide binding site of different enzymes, some of them could be identified also in the sequence of the large subunit of transhydroxylase. In contrast to most enzymes of the DMSO reductase family, transhydroxylase has neither a A,B,C-structure nor a signal sequence, and is not anchored in the cell membrane, but is in the cytoplasm.

While the large subunit has relatively few cysteines which are not clustered, the small subunit has 13 cysteines, some of which are clustered. This makes it likely that the Fe–S centers are located on the small subunit, while the entire MGD cofactor is associated with the large subunit.

For heterologous expression the transhydroxylase gene was cloned into two different expression vectors, the pT7-7 [50] for expression of the wild-type enzyme and pQE30 (Qiagen) for a N-terminal his-tagged enzyme. The C-terminal his-tagged enzyme was obtained by mutagenesis of the pT7-7 (wild-type THL) vector using PCR. In all cases, the expression of transhydroxylase produced inclusion bodies in large amounts which were insoluble, except by cooking with SDS (yielding up to 40% transhydroxylase relative to the total amount of proteins

Table 3

Comparison of transhydroxylase from *P. acidigallici* with the α-subunits of a selection of molybdoenzymes of the DMSO reductase family

Enzymes	Identity (%)	Homology (%)	Structure/cofactor	Reference
DMSO reductase (*Rhodobacter sphaeroides*)	31	56	α/MGD	[38]
DMSO reductase (*Eschericha coli*)	29	51	αβγ/MGD	[39]
DMSO reductase (*Haemophilus influenza*)	28	49	αβγ/n.s.	[40]
Formate dehydrogenase (*Methanobacterium formicicum*)	27	49	αβγ/MGD	[41]
Nitrate reductase (*Bacillus subtilis*)	23	46	n.s.	[42]
Nitrate reductase Z (*Escherichia coli*)	23	50	αβγ/MGD	[43]
Polysulfide reductase (*Wolinella succinogenes*)	22	49	αβγ/MGD	[44]
Formate dehydrogenase F (*Escherichia coli*)	20	45	αβγ/MGD	[45]
Formate dehydrogenase H (*Escherichia coli*)	19	42	αβγ/MGD	[46]
Nitrate reductase (*Klebsiella pneumoniae*)	19	43	n.s.	[47]
Nitrate reductase (*Alcaligenes eutrophus*)	17	42	n.s.	[48]

The number of gaps amounts to between 20 and 30; n.s., no specification.

Table 4
Contacts between amino acids and Mo-co

Amino acids/position in DMSO reductase of *R. sphaeroides*	GAP-comparison with transhydroxylase	Enzymes analogous to *P. acidigallici*	Known amino acids	Evaluation
Domain II				
Y114 (OH)	V150	Enrg, Enrz	Y, L, V, T	++
W116 (N)	Y152			+
S118 (O,g)	H154		S, M, A, C	−
N434 (N)	P499			+
H438 (N,d1)	T503	Efdh, Wdsr	H, R, T, Q, P, S	++
Q440 (N,e2)	T505	Wdsr	Q, S, N, P, A, T	++
Q458 (O)	Q525			+++
D459 (O,d1;O,d2)	S526		D, E, Y	−
D511 (O,d1;O,d2)	D589	highly conserved	D, I, G	+++
Domain III				
S147 (O,g)	H180		S, M, A, C	−
K190 (N)	E220		E, K, N, R, Q, D	++
T191 (O)	T221			+++
I220 (O)	I248			+++
N221 (O,d1;N,d2)	D249	conserved	D, N, S, T, E	++
Q241 (N)	G269			+
D243 (O,d1;O,d2)	D271	highly conserved	D, N	+++
W322 (N)	G355			+
S323 (O,g)	G356	conserved	G, S, C, R	++
R326 (N,h1;N,h2)	R359			+++
Domain IV				
A641 (O)	S736			+
H643 (N,e2;N,d1)	H738	conserved	H, Q, R, P	+++
P644 (O)	P739			+++
R647 (O)	S742			+
H649 (N)	H744			+++
S650 (N;O,g)	T745	Efdn, Wdsr	S, T, A, C	+
Q651 (N,e2)	M746		Q, T, R, W, G	−
E715 (O,e1)	E818	conserved	E, T, Q, V, F	+++
N737 (O,d1;N,d2)	N840	highly conserved	N	+++
G754 (O)	N857			+
Q755 (N,e2)	N858	Ebsr	H, Q, N, R, K	+

Column 1 shows the amino acids and the atoms of the domains II–IV of DMSO reductase from *Rh. sphaeroides* having contact with Mo-co. Column 2 shows the corresponding amino acids in transhydroxylase from *P. acetylenicus*, found by GAP. Column 3 indicates the degree of preservation, or enzymes having at these positions identical amino acids as transhydroxylase (Enrg, nitrate reductase G from *E. coli*; Enrz, nitrate reductase Z from *E. coli*; Efdh, formate dehydrogenase H from *E. coli*; Wdsr, polysulfide reductase from *Wolinella succinogenes*; Efdn, formate dehydrogenase N from *E. coli*; and Ebsr, biotin-sulfoxide reductase from *E. coli*). The next column indicates amino acids found in other enzymes. The further left the amino acid emerges in the series, the more frequently does it occur at the given position. Evaluation indicates the degree of the preservation; +++, identical to DMSO reductase from *R. sphaeroides*; ++, deviation from column 1; however, identity with other molybdoenzymes; +, this amino acid deviates, but contact in *R. sphaeroides* occurs only with atoms of the protein backbone; thus, the remainder of the amino acid is not crucial for the MGD linkage; −, no agreement.

in *E. coli*). Several attempts to express, resolve or refold the transhydroxylase into the catalytically active form, were as yet unsuccessful. The possibility that a shortage of MGD is responsible for the formation of inclusion bodies was also considered. On the one hand nitrate reductase, which is a natural molybdoenzyme of *E. coli* was induced by addition of nitrate, but without any effect to the solubility or activity of the transhydroxylase.

3.3. EPR spectroscopic properties

Below 30 K, the EPR spectrum of the enzyme (as isolated in the presence of air) showed a typical [3Fe–4S] signal with $g_{av} = 2.01$, and a Mo(V) signal at $g \approx 1.98$. The intensity of the [3Fe–4S] resonance corresponded to ≤ 0.1 spins per molecule. Most likely it originated from a slightly acid-labile [4Fe–4S] cluster as previously described for DMSO reductase [18]. This signal was absent in transhydroxylase which had been prepared by a slightly modified procedure which included rapid neutralization of the enzyme fractions after chromatofocussing [35,36]. Above 35 K, the [3Fe–4S] signal disappeared because of relaxation broadening, and a pure Mo(V) 'resting' signal with hyperfine coupling from ^{95,97}Mo remained. Stepwise reduction of the transhydroxylase with sodium dithionite led to an increase of the Mo(V) signal and the disappearance of the [3Fe–4S] resonance at $g_{av} = 2.01$. Upon further addition of reductant two intense new signals appeared with $g_z = 2.08$, $g_y = 1.946$ and $g_x = 1.869$, and $g_z = 2.057$, $g_y = 1.957$ and $g_x = 1.874$, which are characteristic for Fe–S centers (Fig. 3). The first signal broadened

above 30 K, whereas the paramagnetic center with $g_z = 2.057$, $g_y = 1.957$ and $g_x = 1.874$ remained visible up to 70 K. To rule out a possible magnetic interaction between Mo(V) and the Fe–S centers which would influence their relaxation properties, microwave power saturation studies of the Mo(V) signal have been carried out. Comparison of $P_{1/2}$ values of EPR signals of (1) transhydroxylase as isolated, (2) transhydroxylase with only Mo(V) and the fast relaxing Fe–S site (g-values 2.08, 1.946 and 1.869) present, and (3) transhydroxylase with Mo(V) and both paramagnetic Fe–S sites present did not reveal any significant influence of the paramagnetic Fe–S centers on the Mo(V) EPR signal with regard to relaxation or lineshape. It is concluded that there must be at least two different types of [4Fe–4S] centers present in transhydroxylase. Furthermore, the existence of [2Fe–2S] sites cannot be excluded at this stage.

Reichenbecher et al. [36] suggested, on the basis of inhibition experiments with cyanide, that unlike xanthine oxidase or aldehyde oxidase, transhydroxylase most likely contains a MoO_2 site. This idea receives further support from a comparison of the Mo(V) EPR spectra of: (1) enzyme as isolated; (2) enzyme treated with KCN; and (3) enzyme treated with Na_2S. Under these conditions, removal or reinsertion of cyanolyzable sulfur at the Mo center should have induced significant changes of g-values and hyperfine parameters of the Mo(V) site which was not detected.

4. Xanthine oxidase family

The xanthine oxidase family probably is the largest and most diverse family of Mo-co-containing enzymes, with members from eukaryotic, eubacterial, and archaeal sources. Among the members of this family are enzymes which are also found in humans such as xanthine oxidase/dehydrogenase and aldehyde oxidase [51,52]. Bacterial examples are *D. gigas* aldehyde oxidoreductase, the only structurally characterized member of the xantine oxidase family, 4-hydroxylbenzoyl-CoA reductase from both *Rhodopseudomonas palustris* [71] and *Thauera aromatica* [72], quinoline 2-oxidoreductase, quinaldine 4-oxidase, and isoquinoline 1-oxidoreductase [73], and
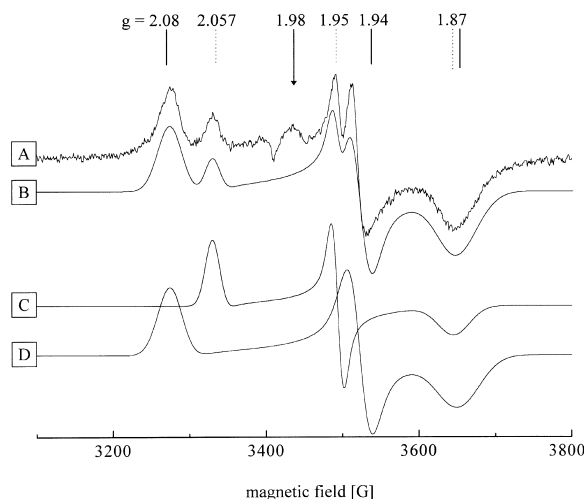

Fig. 3. EPR spectra (X-band, 14 K, 0.6 mW microwave power) of transhydroxylase from *P. acidigallici* reduced with sodium dithionite. (A) Enzyme as isolated, 4.3 mg/ml in 40 mM TEA buffer, 300 mM NaCl, pH 7.3, after addition of 3.5 equivalents sodium dithionite, under anoxic conditions. (B) Combined simulations, with signals C and D, weight 2:3. (C) Simulated spectrum, with $g_x = 1.874$, $g_y = 1.953$, $g_z = 2.057$. (D) Simulated spectrum, with $g_x = 1.869$, $g_y = 1.940$, $g_z = 2.080$.

several CO dehydrogenases. A conserved feature of this family appears to be the presence of a non-protein sulfur ligand of the molybdenum which can be removed from the enzyme by treatment with cyanide. Prior to the crystal structure of *D. gigas* aldehyde oxidoreductase, the general architecture of most members of the xanthine oxidase family was believed to be comprised of four domains starting at the N-terminus with two [2Fe–2S] cluster containing domains followed by a flavin binding domain (not present in *D. gigas* aldehyde oxidoreductase), and finally the Mo-co-containing domain giving rise to a total molecular mass of approximately 150 kDa per monomer. A few members of this family have a different genetic architecture in which some of the four domains are encoded by different genes, but the overall structure is expected to be rather similar for all members of this family.

4.1. Structure of D. gigas aldehyde oxidoreductase

The crystal structure of *D. gigas* aldehyde oxidoreductase [10,11] showed that each 907 residue containing subunit of the dimeric enzyme folds into four domains (Fig. 4A). The Mo-co in *D. gigas* aldehyde oxidoreductase consists of a single molecule of a molybdopterin cytosine dinucleotide. However, the Mo-co in xanthine oxidase/dehydrogenase from different sources contains no additional nucleotide. Each of the two N-terminal domains is approximately 75 residues long and is involved in coordination of one of the two [2Fe–2S] clusters. Domain I adopts a fold analogous to that of plant-type [2Fe–2S] ferredoxins consisting of a five-stranded β-sheet and a partially enclosed β-helix, while domain II folds into a four-helix bundle that had not been previously observed to coordinate iron–sulfur clusters. The remainder of the structure was found to consist of two domains rather than one single domain as had been anticipated. These two domains have been designated Mo1 and Mo2 domains and together are responsible for binding the Mo-co. They are considerably larger (386 and 326 residues, respectively) than the two N-terminal domains. The Mo1 domain has substantial β-sheet structure and appears to be organized into two subdomains. The first contains a seven-stranded incomplete β-barrel wrapped around a central β-helix and the second a five-

stranded antiparallel β-sheet. The Mo2 domain also consists of two subdomains, each having an α/β-structure. The Mo1 domain provides most of the binding interactions to the molybdopterin, whereas the Mo2 domain contributes only a few interactions to the molybdopterin, but all of the interactions with the cytosine nucleotide. The Mo-co is buried between the Mo1 and Mo2 domains and access to the active site is provided through a 15-Å-long channel. The FAD domain which is present in all other members of the xanthine oxidase family will probably replace a 38-residue-long peptide which connects the second [2Fe–2S] cluster containing domain and the Mo1 domain. It should be noted that, with the exception of the [2Fe–2S] containing domains, the remaining structure has been classified differently in the SCOP database [53]. Most importantly, residues 311–907 are considered to form one domain, which contains four subdomains arranged in tandem repeat forming a bi-lobed structure (Fig. 4B). Each subdomain contains a predominantly parallel β-sheet packed against two α-helices with the first two and last two subdomains each forming one lobe. This domain mediates all the interactions with the Mo-co and represents a fold that has not been observed in any other protein structure.

4.2. Active site structure

The initial crystal structure of *D. gigas* aldehyde oxidoreductase [11] represented an inactive form of the enzyme in which the non-protein sulfur had been replaced by an oxygen atom leading to a penta-co-ordinated molybdenum center with two sulfur ligands and three oxygen ligands. In the active, sulfur-containing form of the enzyme [10], the Mo was found to be coordinated by the two dithiolene sulfurs of the molybdopterin, an oxo ligand, a water molecule and a sulfido group. The sulfido group occupies the apical position of the square pyramidal arrangement created by the Mo ligands. No Mo ligands are provided from the protein, although the side chain of the conserved Glu-869, which forms a hydrogen bond to the Mo-bound water molecule, is within 3.5 Å of the metal. The overall arrangement of the metal centers is such that the Mo and the second [2Fe–2S] cluster are separated by 15 Å while the two [2Fe–2S] clusters are separated by 12 Å.
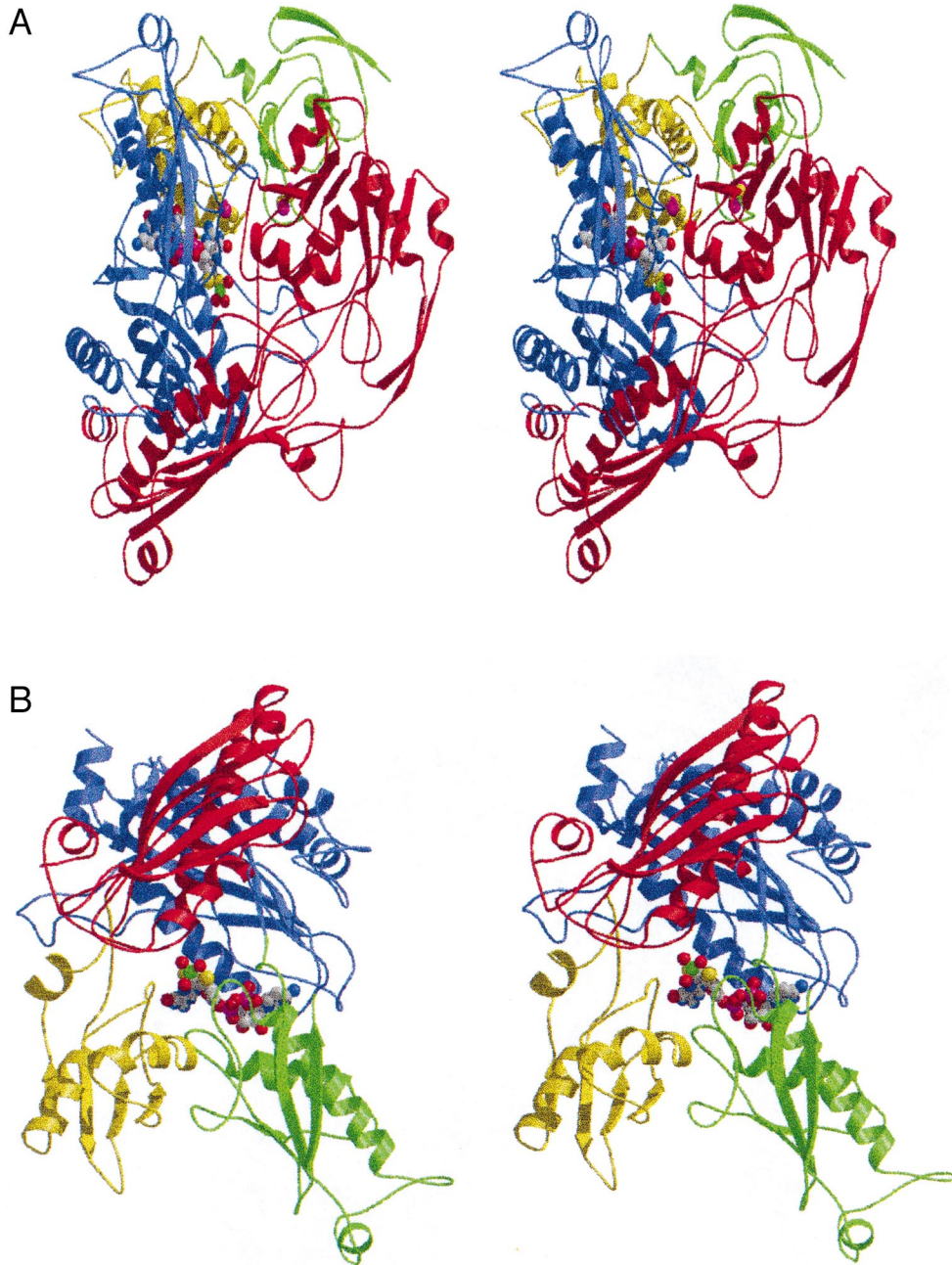
Fig. 4. (A) Schematic ribbons stereo representation of a monomer of aldehyde oxidoreductase from *D. gigas* viewed into the active site with the [2Fe–2S] cluster containing domains in green and yellow, and the Mo1 and Mo2 domains in red and blue, respectively. The cofactors are shown in a space filling representation with the Fe-atoms in purple. (B) Alternative classification of residues 311–907 according to the SCOP database. The four repeating subdomains are shown in yellow, red, green and blue. The yellow and red as well as the green and blue subdomains form one lobe and the two lobes are related by an approximate two-fold axis of symmetry.

However, there are direct interactions between the Mo-co and the second [2Fe–2S] cluster through the side chain of Cys-139 which provides a ligand to the [2Fe–2S] cluster and is, at the same time, hydrogen bonded to the exocyclic amino group of the molybdopterin. This arrangement seems to facilitate electron transfer between the two metal centers. The substrate binding site was inferred from a bound isopropanol molecule, which is located near the equatorial water molecule. Based on the structural studies, a mechanism has been proposed for this enzyme [10]. The key feature of the proposed mechanism is a hydride transfer from the substrate to the sulfido group. According to the crystallographic analysis, there is some partial disulfide bond character between the two dithiolene S-atoms in the oxidized form which is lost upon reduction.

5. Sulfite oxidase family

Sulfite oxidase and the assimilatory nitrate reductases from algae, fungi and higher plants form the third group of Mo-co-containing enzymes. Sulfite oxidase is mainly found in eukaryotes and is located in the mitochondrial intermembrane space where it catalyzes the oxidation of sulfite to sulfate. This is the terminal reaction in the oxidative degradation of the sulfur-containing amino acids cysteine and methionine. Sulfite oxidase has been characterized so far from human [54], rat [55], bovine and chicken [56], and from one prokaryote, *Thiobacillus novellus* [57] In all cases, the enzyme was found to be a homodimer with a molecular mass between 101 and 110 kDa. The rat enzyme can be proteolytically cleaved into two fragments [58]: a small N-terminal fragment of about 10 kDa containing a b_5 cytochrome, and a large C-terminal fragment, about 42 kDa, which harbors the molybdenum cofactor. Assimilatory nitrate reductases catalyze the reduction of nitrate to nitrite which is subsequently converted to NH_4^+ by nitrite reductase. Nitrate reductases have been isolated from fungi [59], algae [60], and higher plants [61] and form homodimers with a molecular mass of ~ 220 kDa. In addition to the Mo-co and the b_5 cytochrome present in sulfite oxidases, these enzymes contain FAD and a binding site for NAD(P)$^+$ [62]. A crystal structure of a fragment of corn nitrate reductase comprising the flavin binding domain has been published [63].

5.1. Overall structure of sulfite oxidase

The recently determined crystal structure of chicken sulfite oxidase at 1.9 Å resolution [16] provides the first complete structural model for any member of this family. The fold of sulfite oxidase can be described as a mixed α+β-structure and is composed of three domains (Fig. 5). Domain I (residues 3–84) is structurally similar to bovine cytochrome b_5 and comprises a three-stranded antiparallel β-sheet and six α-helices. Five α-helices and the β-sheet form a hydrophobic crevice in which the heme group is deeply buried with the vinyl groups pointing towards the β-sheet and the propionate side chains to the solvent. The heme iron atom in sulfite oxidase is octahedrally coordinated by the $N_\epsilon 2$ atoms of His-40 and His-65, and the four heme pyrrole nitrogens. Domains I and II are connected by a flexible linker peptide (residues 86–95) which is not well defined in the electron density. Domain II (residues 96–323) contains thirteen β-strands organized in three β-sheets, and nine α-helices and is comprised of a previously unobserved polypeptide fold. At the N-terminus of this domain, a three-stranded antiparallel β-sheet is formed which leads into a mixed five-stranded β-sheet located on the opposite side of the domain. This β-sheet is flanked by five short α-helices. The center of domain II is comprised of a long β-hairpin which, together with two other β-strands, forms a four-stranded antiparallel β-sheet. The Mo-co is bound at the center of the second domain and is contacted by discontinuous stretches of the polypeptide chain. The core of the C-terminal domain (residues 324–466) is characterized by seven β-strands arranged in two antiparallel β-sheets. Structural comparisons revealed that this domain shares structural similarity with the C2 subtype of the immunoglobulin superfamily. As expected, the enzyme s present as a dimer in the crystal with overall dimensions of $120 \times 55 \times 70$ Å^3 and the dimer interactions are mediated almost exclusively through the third domains in a head-to-head arrangement.
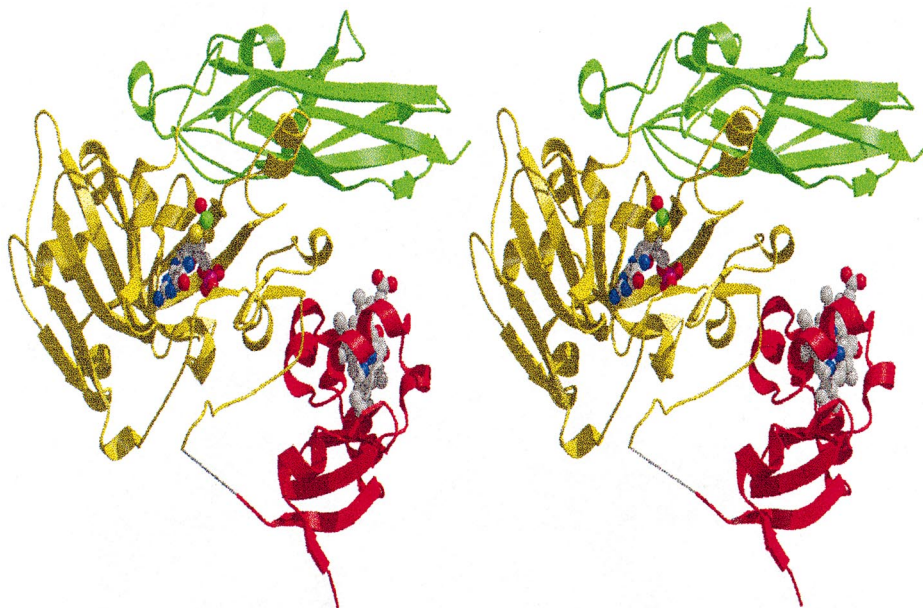
Fig. 5. Crystal structure of sulfite oxidase. Ribbons representation of the polypeptide fold of the monomer with domains I, II and III in red, yellow and green, respectively. The cofactors are shown in a space filling representation.

5.2. Active site structure

The active site of sulfite oxidase comprises the Mo-co in the form of a single molybdopterin without a second nucleotide. The Mo is coordinated by the dithiolene sulfurs of the molybdopterin and by a cysteine side chain (Cys-185) from the protein. Two additional ligands to the Mo have been identified in the crystal structure: an oxo group and a water or hydroxide. The latter ligand is at a distance of 2.3 Å and therefore it is somewhat more likely to be a water molecule, but a definitive assignment could not be made. The geometry of the ligands can be described as square pyramidal with the oxo group occupying the apical position. The observed coordination geometry is at variance with the dioxo Mo center postulated by EXAFS spectroscopy [64] and it seems possible that the crystal structure represents a reduced form of the enzyme. Reduction could have occurred through traces of sulfite present in the crystallization medium (1.0 M Li_2SO_4) or through photoreduction in the X-ray beam. A sulfate has been identified in close proximity to the Mo-co, with a distance of 5.1–5.2 Å between the Mo and the S. The sulfate is bound in an anion binding pocket

equally suited to accommodate the substrate sulfite and the product sulfate, and its negative charge is neutralized by the positively charged side chains Arg-138, Arg-190, Arg-450 and Lys-200. The equatorial water/hydroxyl ligand of the Mo is located between the metal and the bound SO_4^{2-}. The one oxygen in the bound sulfate that has a weaker electron density indicates that a bound sulfite would be oriented such that its sulfite lone pair is pointing roughly toward the water/hydroxy ligand. In the oxidized form of the enzyme this water/hydroxyl is probably replaced by a second oxo-group. The crystal structure suggests that the oxygen atom in the equatorial position is being transferred from the Mo to the substrate. However, a postulated bidentate intermediate in which the transferred oxygen is bridging the Mo and the sulfur would require the substrate to bind even closer to the Mo than the bound sulfate.

6. Aldehyde ferredoxin oxidoreductase family

Aldehyde ferredoxin oxidoreductase (AOR) catalyzes the interconversion of aldehydes and carboxy-

lates and was the first member of this family to be discovered and the first enzyme containing this co-factor to be characterized by X-ray crystallography [9]. Other members of the AOR family include form-aldehyde ferredoxin oxidoreductase (FOR) and glyc-eraldehyde-3-phosphate ferredoxin oxidoreductase (GAPOR) isolated from the hyperthermophilic or-ganism *P. furiosus*, a carboxylic acid reductase found in certain acetogenic *clostridia*, an aldehyde dehydro-genase from *D. gigas* which is unrelated to the alde-hyde oxidoreductase isolated from the same organ-ism and hydroxycarboxylate viologen oxidoreductase from *Proteus vulgaris*. With the exception of the last enzyme, all members of this family are tungsten-con-taining enzymes.

6.1. Overall structure of aldehyde oxidoreductase

AOR is a dimer of two identical 605 residue sub-units and the 2.3 Å crystal structure [9] has shown that each subunit is folded into three domains (Fig. 6). Domain I (residues 1 to 210) consists of two six-stranded β-sheets which are arranged into a 12-stranded open anti-parallel β-barrel. Domain I forms a base on which the saddle-like tungsten pterin co-factor sits, which in this case consists of two pterins

with no additional nucleotide. The fold of domain I exhibits a pseudo two-fold axis that coincides ap-proximately with a two-fold axis passing through the tungsten also relating the two molybdopterins. Domains II and III (residues 211–417 and residues 418–605, respectively) mostly contain α-helices and are roughly related by the two-fold axis described above. Each of these domains contains an Asp-X-X-Gly-Leu-(Cys or Asp)-X sequence motif which participates in the binding of one pterin. The first four residues within each motif form a β-turn, and the side chain of the first Asp and the main chain oxygen of the Leu contact the exocyclic amino group of each pterin. Domain III harbors a [4Fe–4S] clus-ter which, besides a mononuclear metal ion located on the dyad axis of the AOR dimer, is the additional cofactor present in this enzyme. A long hydrophobic channel is formed at the interface between domains II and III and provides access to the active site. Domain I as well as the C-terminal domains have polypeptide folds that have not been observed in other protein structures.

6.2. Active site structure
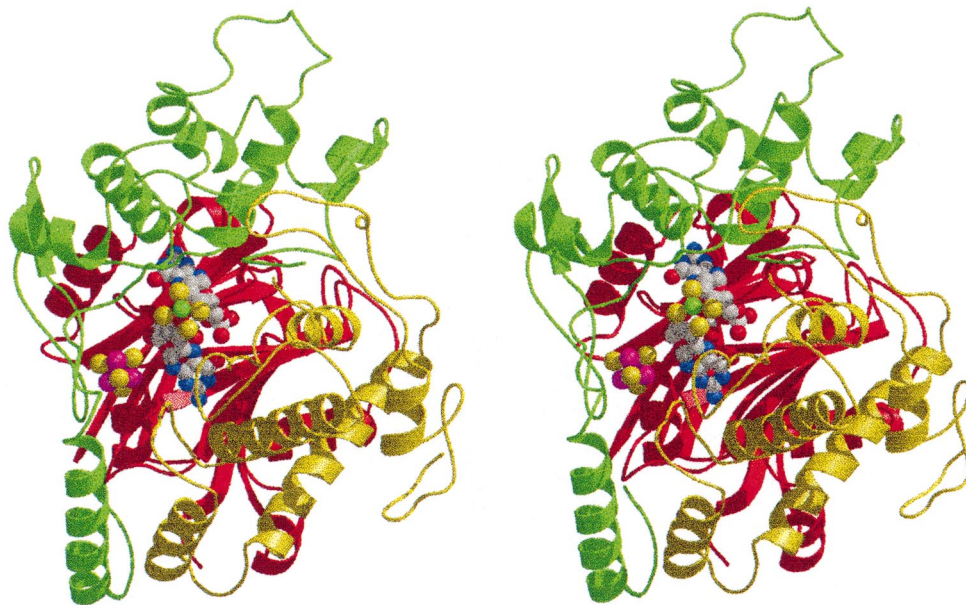
The tungsten in AOR is symmetrically coordi-

Fig. 6. Structure of aldehyde ferredoxin oxidoreductase. Stereoview of α-ribbons representation of an AOR monomer viewed into the ac-tive site with domains I, II and III in red, green and yellow, respectively. The cofactors are shown in ball-and-stick representation.

nated by the four dithiolene sulfurs from the two molybdopterins and the arrangement of the tungsten and the dithiolene sulfurs can be described as distorted square pyramidal. The presence and location of oxo/hydroxo groups coordinated to the tungsten could not be definitely established crystallographically, perhaps due to either disorder at this center, or crystallographic problems associated with locating light atoms in the vicinity of heavy metals [26]. No protein ligands to the tungsten have been observed, which, besides the overall differences in the polypeptide structure, clearly distinguishes this family from the DMSO reductase family. However, the side chains of residues Glu-313 and His-448 are in the vicinity of the tungsten and could participate in proton transfer reactions coupled to electron transfer. The [4Fe–4S] cluster is in close proximity (approximately 8 Å) to the tungsten cofactor. As in *D. gigas* aldehyde oxidoreductase and formate dehydrogenase H, one of the pterins seems to be involved in electron transfer, since Cys-494, a [4Fe–4S] cluster ligand, is also hydrogen bonded to one of the pterins, thus providing a direct link between these two cofactors. An additional feature in AOR is the presence of a magnesium ion which is located below the tungsten, on the two-fold axis passing through the cofactor. The magnesium ion exhibits octahedral coordination geometry and interacts with the two terminal phosphates of the cofactor, two water molecules and two backbone carbonyl oxygens. At present, little is known about the mechanistic details of AOR or any member of this family. Thus it is also unclear whether AOR catalyzes its reaction through an oxo-group or hydride transfer mechanism. Additional complications arise from the fact that the isolated form of AOR in dithionite contains a mixture of several oxidation states with the W(IV), W(V) and W(VI) states all being present.

7. Acetylene hydratase from *P. acetylenicus*

7.1. Molecular properties and reactivity

Acetylene hydratase was recently purified from *P. acetylenicus* and characterized as an iron–sulfur tungsten enzyme [65]. It represents the only member of a third class of tungsten enzymes besides the aldehyde oxidoreductase family and the formyl-methanofuran dehydrogenase family [8,65,66]. Acetylene hydratase catalyzes the hydration of acetylene to acetaldehyde: $H–C\equiv C–H + H_2O \rightarrow H_3C–CHO$ ($\Delta G_o' = -119$ kJ mol^{-1}).

This is not a redox reaction and differentiates acetylene hydratase from other tungsten enzymes known so far. In the photometric assay which is coupled to alcohol dehydrogenase/NADH (conversion of acetaldehyde to ethanol), a strong reductant, such as titanium(III)-citrate [67], or dithionite, has to be used to obtain maximum activity (≈ 3.5 units/mg protein) [65]. From redox titrations of the enzyme a lower limit of ≈ -330 mV was determined to observe activity.

Acetylene hydratase is a monomeric enzyme, with a molecular mass of 72 kDa (SDS-PAGE), and 83 kDa (MALDI). In the MALDI experiments, acetylene hydratase showed a single sharp peak at $83\,212 \pm 100$ Da under denaturing conditions, at pH 2.0; under non-denaturing conditions, pH 6.2, the main peak was much broader because of several subspecies. One major peak appeared at 83 554 Da corresponding to the addition of one [4Fe–4S] center, and another major peak at 84 999 Da corresponding to the addition of one [4Fe–4S] and one Mo(MGD)$_2$ unit. So far, 19 amino acids of the N-terminus have been sequenced. There was no homology to any protein in the data bank except for a X-C-X-C-C-X-X-X-C-X sequence which could represent a motif for a Fe–S site [65]. 4.4 ± 0.4 mol Fe and 0.5 ± 0.1 W (ICP/MS), 3.9 ± 0.4 mol acid labile sulfur and 1.3 ± 0.1 molybdopterin guanine-dinucleotide cofactor were found per mol enzyme. Selenium was absent. The analytical data point towards a coordination of the tungsten center similar to that observed in *R. capsulatus* DMSO reductase [12], formate dehydrogenase (FDH$_H$) from *Escherichia coli* [15], or AOR of *P. furiosus* [9]. In these enzymes tungsten, or molybdenum, is coordinated by the four dithiolene sulfur atoms as discussed earlier. There is no selenocysteine as reported for FDH$_H$ from *E. coli* [68], and coordinated oxo groups from serine as in DMSO reductase from *Rhodobacter capsulatus* [12] appear unlikely to be bound to tungsten in view of the high g_{av} as discussed below. However, the presence of a pterin

guanine dinucleotide cofactor differentiates AH from the AOR family, where all members have a pterin mononucleotide cofactor.

Most recently, a fully active acetylene hydratase was obtained from *P. acetylenicus* cells which had been grown in the absence of tungsten. Surprisingly, a molybdenum-containing form of the enzyme could be purified, with identical molecular mass (SDS), and the first 10 amino acids of the N-terminus were also identical. ICP/MS clearly demonstrated the presence of molybdenum, whereas tungsten was absent in this active form of the enzyme. The redox properties of the molybdenum acetylene hydratase, however, were different. This form of the enzyme was inactive under the strongly reducing conditions used for tungsten acetylene hydratase. For maximum activity, the molybdenum enzyme had to be reduced with a small amount of either dithionite or Ti(III)-citrate, but the activity dropped sharply upon further reduction in contrast to the tungsten enzyme.

7.2. EPR spectroscopic properties

EPR spectra of acetylene hydratase (as isolated, in the presence of air) showed the typical signal of a [3Fe–4S] cluster with $g_{av} = 2.01$, at 10 K; this signal was absent in enzyme prepared under the exclusion of air. Upon reduction with dithionite, a rhombic signal appeared with resonances at $g_z = 2.048$, $g_y = 1.939$, and $g_x = 1.920$ indicative of a low potential ferredoxin type [4Fe–4S] cluster [69]. Note that addition of dithionite did not lead to the generation of an EPR signal typical for W(V). Upon titrating the enzyme with the oxidant hexacyanoferrate(III), a new signal appeared with $g_x = 2.007$, $g_y = 2.019$, and $g_z = 2.048$ ($g_{av} = 2.022$). This signal disappeared upon further addition of hexacyanoferrate(III). It showed a temperature optimum around 5 K under non-saturating conditions of microwave power, and was still visible at 150 K, thus was tentatively assigned to the W(V) center. Signals with comparably high g-values had been reported earlier for *E. coli* FDH$_H$ where a selenocysteine residue acts as a ligand to the tungsten [68].

These preliminary data suggest a tungsten, or a molybdenum center, coordinated by four dithiolene sulfur atoms at the catalytic site. The role of the [4Fe–4S] cluster remains unclear at this moment.

Most recently, model studies with a W(IV) complex, but not the corresponding W(VI) complex, demonstrated the likely participation of a reduced tungsten pterin cofactor moiety for catalyzing the hydration of acetylene [70].

8. Structural comparison

The crystal structures of Mo-co-containing enzymes have revealed a remarkable degree of structural diversity in the overall polypeptide folds as well as in the composition and stoichiometry of the Mo-co. Based on the available data, a few structural features seem noteworthy:

1. The structures of Mo-co-containing enzymes representing the four different enzyme families indicate that there seems to be no ancestral Mo-co-containing enzyme from which all enzymes containing this cofactor derived. Instead, evolution independently selected at least four different protein folds to harbor the Mo-co.

2. Some of the polypeptide folds found in Mo-co-containing enzymes have until now never been observed in other proteins. For instance, the Mo-co-containing domains in *D. gigas* aldehyde oxidoreductase and sulfite oxidase as well as domain I and the C-terminal domains of AOR represent novel polypeptide folds.

3. All enzymes consist of at least three structural domains and in some cases differences between different family members are reflected by the addition or removal of individual domains. For instance, the assimilatory nitrate reductases differ from sulfite oxidase by insertion of an additional cytochrome reductase domain.

4. In all cases, the Mo-co is deeply buried in the enzyme and access to the active site is usually provided by channels or funnels.

5. All crystal structures revealed that the molybdopterin is present in a tricyclic form with a pyran ring fused to the pterin nucleus. The pyran ring is generated through nucleophilic attack of the 3′-OH group on C7 of the pterin moiety.

6. There is considerable variation between different families in the stoichiometry of the molybdopterin. Two copies of the molybdopterin are present in the DMSO reductase and AOR families, whereas only one copy is found in the sulfite oxidase and xanthine oxidase families.

7. Amino acid side chains coordinating the molybdenum do occur in two of the four families. In the DMSO reductase family this side chain is either a Ser, a Cys, or a Seleno-Cys, whereas it is always a Cys in the sulfite oxidase family.

8. With the exception of sulfite oxidase, the molybdopterin is oriented in such a way that it can participate directly in electron transfer between the Mo/W and additional cofactors. Such an arrangement has been observed in the crystal structures of AOR, *D. gigas* aldehyde oxidoreductase and formate dehydrogenase H.

9. There is additional variation of the molybdopterin regarding the presence of a dinucleotide form of the cofactor, even within the same family as is seen for *D. gigas* aldehyde oxidoreductase (dinucleotide form) and xanthine oxidase (no additional nucleotide). The role of the additional nucleotide remains unclear and so far no functional role has been assigned to it.

Acknowledgments

References

[1] Enemark, J.H. and Young, C.G. (1993) Bioinorganic chemistry of pterin-containing molybdenum and tungsten enzymes. Adv. Inorg. Chem. 40, 1–88.

[2] Hille, R. (1994) The reaction mechanism of oxomolybdenum enzymes. Biochim. Biophys. Acta 1184, 143–169.

[3] Hille, R. (1996) The mononuclear molybdenum enzymes. Chem. Rev. 96, 2757–2816.

[4] Wootton, J.C., Nicholson, R.E., Cock, J.M., Walters, D.E., Burke, J.F., Doyle, W.A. and Bray, R.C. (1991) Enzymes depending on the pterin molybdenum cofactor: sequence families, spectroscopic properties and possible cofactor-binding domains. Biochim. Biophys. Acta 1057, 157–185.

[5] Rajagopalan, K.V. (1991) Novel aspects of the biochemistry of the molybdenum cofactor. Adv. Enzym. 64, 215–290.

[6] Rajagopalan, K.V. and Johnson, J.L. (1992) The pterin molybdenum cofactors. J. Biol. Chem. 267, 10199–10202.

[7] Johnson, J.L., Rajagopalan, K.V., Mukund, S. and Adams, M.W.W. (1993) Identification of molybdopterin as the organic component of the tungsten cofactor in four enzymes from hyperthermophilic archaea. J. Biol. Chem. 268, 4848–4852.

[8] Johnson, M.K., Rees, D.C. and Adams, M.W.W. (1996) Tungstoenzymes. Chem. Rev. 96, 2817–2839.

[9] Chan, M.K., Mukund, S., Kletzin, A., Adams, M.W.W. and Rees, D.C. (1995) Structure of a hyperthermophilic tungstopterin, aldehyde ferredoxin oxidoreductase. Science 267, 1463–1469.

[10] Huber, R., Hof, P., Duarte, R.O., Moura, J.J.G., Moura, I., Liu, M.-Y., LeGall, J., Hille, R., Archer, M. and Romão, M.J. (1996) A structure-based catalytic mechanism for the xanthine oxidase family of molybdenum enzymes. Proc. Natl. Acad. Sci. USA 17, 8846–8851.

[11] Romão, M.J., Archer, M., Moura, I., LeGall, J., Engh, R., Schneider, M., Hof, P. and Huber, R. (1995) Crystal structure of the xanthine oxidase-related aldehyde oxido-reductase from *Desulfovibrio gigas*. Science 270, 1170–1176.

[12] Schindelin, H., Kisker, C., Hilton, J., Rajagopalan, K. V. and Rees, D.C. (1996) Crystal structure of DMSO reductase: redox-linked changes in molybdopterin coordination. Science 272, 1615–1621.

[13] McAlpine, A.S., McEwan, A.G., Shaw, A.L. and Bailey, S. (1997) Molybdenum active centre of DMSO reductase from *Rhodobacter capsulatus*: crystal structure of the oxidised enzyme at 1.82 Å resolution and the dithionite-reduced enzyme at 2.8 Å resolution. J. Biol. Inorg. Chem. 2, 690–701.

[14] Schneider, F., Löwe, J., Huber, R., Schindelin, H., Kisker, C. and Knäblein, J. (1996) Crystal structure of dimethyl sulfoxide reductase from *Rhodobacter capsulatus* at 1.88 Å resolution. J. Mol. Biol. 263, 53–69.

[15] Boyington, J.C., Gladyshev, V.N., Khangulov, S.V., Stadtman, T.C. and Sun, P.D. (1997) Crystal structure of formate

dehydrogenase H: catalysis involving Mo, molybdopterin, selenocysteine, and an Fe_4S_4 cluster. Science 275, 1305–1308.

[16] Kisker, C., Schindelin, H., Pacheco, A., Wehbi, W.A., Garrett, R.M., Rajagopalan, K.V., Enemark, J.H. and Rees, D.C. (1997) Molecular basis of sulfite oxidase deficiency from the structure of sulfite oxidase. Cell 91, 973–983.

[17] Kisker, C., Schindelin, H. and Rees, D.C. (1997) Molybdenum-cofactor containing enzymes: structure and mechanism. In: Annual Reviews in Biochemistry (Richardson, C.C., Ed.), pp. 233–267. Annual Reviews, Palo Alto.

[18] Weiner, J.H., Rothery, R.A., Sambasivarao, D. and Trieber, C.A. (1992) Molecular analysis of dimethylsulfoxide reductase: a complex iron–sulfur molybdoenzyme of Escherichia coli. Biochim. Biophys. Acta 1102, 1–18.

[19] Satoh, T. and Kurihara, F.N. (1987) Purification and properties of dimethylsulfoxide reductase containing a molybdenum cofactor from a photodenitrifier, Rhodopseudomonas sphaeroides f.s. denitrificans. J. Biochem. 102, 191–197.

[20] McEwan, A.G., Ferguson, S.J. and Jackson, J.B. (1991) Purification and properties of dimethyl-sulfoxide reductase from Rhodobacter capsulatus – a periplamic molybdoenzyme. Biochem. J. 274, 305–307.

[21] McAlpine, A.S., McEwan, A.G. and Bailey, S. (1998) The high resolution crystal structure of DMSO reductase in complex with DMSO. J. Mol. Biol. 275, 613–623.

[22] Kraulis, P.J. (1991) MOLSCRIPT – a program to produce both detailed and schematic plots of protein structures. J. Appl. Cryst. 24, 946–950.

[23] Bacon, D.J. and Anderson, W.F. (1988) A fast algorithm for rendering space-filling molecule pictures. J. Mol. Graph. 6, 219–220.

[24] Merritt, E.A. and Murphy, M.E.P. (1994) Raster3D Version 2.0 – a program for photorealistic molecular graphics. Acta Cryst. D50, 869–873.

[25] Schulz, G.E. (1992) Binding of nucleotides by proteins. Curr. Opin. Struct. Biol. 2, 61–67.

[26] Ludvigsen, S. and Poulsen, F.M. (1992) 3-Dimensional structure in solution of barwin, a protein from barley seed. Biochemistry 31, 8783–8789.

[27] Davies, G.J., Dodson, G.G., Hubbard, R.E., Tolley, S.P., Dauter, Z., Wilson, K.S., Hjort, C., Mikkelsoen, J.M., Rasmussen, G. and et al. (1993) Structure and function of endoglucanase V. Nature 365, 362–364.

[28] George, G.N., Hilton, J. and Rajagopalan, K.V. (1996) X-ray absorption spectroscopy of dimethylsulfoxide reductase from Rhodobacter sphaeroides, J. Am. Chem. Soc. 118, 1113–1117.

[29] Baugh, P.E., Garner, C.D., Charnock, J.M., Collison, D., Davies, E.S., McAlpine, A.S., Bailey, S., Lane, I., Hanson, G.R. and McEwan, A.G. (1997) X-ray absorption spectroscopy of dimethylsulfoxide reductase from Rhodobacter capsulatus, J. Biol. Inorg. Chem. 2, 634–643.

[30] Bennett, B., Benson, N., McEwan, A.G. and Bray, R.C. (1994) Multiple states of the molybdenum centre of dimethylsulphoxide reductase from Rhodobacter capsulatus revealed by EPR spectroscopy. Eur. J. Biochem. 225, 321–331.

[31] Schindelin, H., Kisker, C. and Rees, D.C. (1997) The molybdenum-cofactor: a crystallographic perspective. J. Biol. Inorg. Chem. 2, 773–781.

[32] George, G.N., Colangelo, C.M., Dong, J., Scott, R.A., Kangulov, S.V., Gladyshev, V.N. and Stadtman, T.C. (1998) X-ray absorption spectroscopy of the molybdenum site of Escherichia coli formate dehydrogenase. J. Am. Chem. Soc. 120, 1267–1275.

[33] Khangulov, S.V., Gladyshev, V.N., Dismukes, G.C. and Stadtman, T.C. (1998) Selenium-containing formate dehydrogenase H from Escherichia coli: a molybdopterin enzyme that catalyzes formate oxidation without oxygen transfer. Biochemistry 57, 3518–3528.

[34] Schink, B. and Pfennig, N. (1992) Fermentation of trihydroxybenzenes by Pelobacter acidigallici gen. nov. Sp. Nov., a new strictly anaerobic, non-fermenting bacterium. Arch. Microbiol. 133, 195–201.

[35] Brune, A. and Schink, B. (1992) Phloroglucinol pathway in the strictly anaerobic Pelobacter acidigallici – fermentation of trihydroxybenzenes to acetate via triacetic acid. Arch. Microbiol. 157, 417–424.

[36] Reichenbecher, W., Brune, A. and Schink, B. (1994) Transhydroxylase of Pelobacter acidigallici – a molybdoenzyme catalyzing the conversion of pyrogallol to phloroglucinol. Biochim. Biophys. Acta 1204, 217–224.

[37] Reichenbecher, W., Rüdiger, A., Kroneck, P.M.H. and Schink, B. (1996), One molecule of molybdopterin guanine dinucleotide is associated with each subunit of the heterodimeric Mo–Fe–S protein transhydroxylase of Pelobacter acidigallici as determined by SDS/PAGE and mass spectrometry. Eur. J. Biochem. 237, 406–413.

[38] Yamamoto, I., Wada, N., Ujiiye, T., Tachibana, M., Matsuzaki, M., Kajiwara, H., Watanabe, Y., Hirano, H. and Okubo, A. (1995) Cloning and nucleotide sequence of the gene encoding dimethyl sulfoxide reductase from Rhodobacter sphaeroides f.s. denitrificans, Biosci. Biotechnol. Biochem. 59, 1850–1855.

[39] Bilous, P.T., Cole, S.T., Anderson, W.F. and Weiner, J.H. (1988) Nucleotide sequence of the dmsABC operon encoding the anaerobic dimethyl sulfoxide reductase of Escherichia coli. Mol. Microbiol. 2, 785–795.

[40] Fleischmann, R.D., Adams, M.D., White, O., Clayton, R.A., Kirkness, E.F., Kerlavage, A.R., Bult, C.J., Tomb, J.-F., Dougherty, B.A., Merrick, J.M., McKenney, K., Sutton, G. et al. (1995) Whole genome random sequencing and assembly of Haemophilus influenzae. Science 269, 496–512.

[41] Shuber, A.P., Orr, E.C., Recny, M.A., Schendel, P.F., May, H.D., Schauer, N.L. and Ferry, J.G. (1986) Cloning, expression and nucleotide sequence of the formate dehydrogenase genes from Methanobacterium formicicum. J. Biol. Chem. 261, 12942–12947.

[42] Hoffmann, T., Troub, B., Szabo, A., Hungerer, C. and Jahn, D. (1995) The anaerobic life of Bacillus subtilis: cloning of the genes encoding the respiratory nitrate reductase system, FEMS Microbiol. Lett. 133, 219–225.

[43] Blasco, F., Iobbi, C., Ratouchniak, J., Bonnefoy, V. and Chippaux, M. (1990) Nitrate reductases of Escherichia coli: sequence of the second nitrate reductase and comparison

with that encoded by the *narGHJI* operon. Mol. Gen. Genet. 222, 104–111.

[44] Kraft, T., Bokranz, M., Klimmek, O., Schroeder, I., Fahrenholz, F., Kojro, E. and Kröger, (1992) Cloning and nucleotide sequence of the psrA gene of *Wolinella succinogenes* polysulphide reductase. Eur. J. Biochem. 206, 503–510.

[45] Plunkett, G., III, Burland, V.D., Daniels, D.L. and Blattner, F.R. (1993) Analysis of the *Escherichia coli* genome. III. DNA sequence of the region from 87.2 to 89.2 minutes. Nucleic Acids Res. 21, 3391–3398.

[46] Berg, B.L., Li, J., Heider, J. and Stewart, V. (1991) Nitrate-inducible formate dehydrogenase in *Escherichia coli* K-12. I. Nucleotide sequence of the *fdnGHI* operon and evidence that opal (UGA) encodes selenocysteine. J. Biol. Chem. 266, 22380–22385.

[47] Lin, J.T., Goldman, B.S. and Stewart, V. (1993) Structures of genes *nasA* and *nasB*, encoding assimilatory nitrate and nitrite reductases in *Klebsiella pneumoniae* M5al, J. Bacteriol. 175, 2370–2378.

[48] Siddiqui, R.A., Warnecke-Eberz, U., Hengsberger, A., Schneider, B., Kostka, S. and Friedrich, B. (1993) Structure and function of a periplasmic nitrate reductase in *Alcaligenes eutrophus* H16. J. Bacteriol. 175, 5867–5876.

[49] Devereux, J., Haeberli, P. and Smithies, O. (1984) A comprehensive set of sequence analysis programs for the VAX. Nucleic. Acids Res. 12, 387–395.

[50] Tabor, S. and Richardson, C.C. (1985) A bacteriophage T7 RNA polymerase/promoter system for controlled exclusive expression of specific genes. Proc. Natl. Acad. Sci. USA 82, 1074–1078.

[51] Turner, N.A., Doyle, W.A., Ventom, A.M. and Bray, R.C. (1995) Properties of rabbit liver aldehyde oxidase and the relationship of the enzyme to xanthine oxidase and dehydrogenase. Eur. J. Biochem. 232, 646–657.

[52] Romão, M.J. and Huber, R. (1998) Structure and function of the xanthine-oxidase family of molybdenum enzymes. Struct. Bond. 90, 69–95.

[53] Murzin, A.G., Brenner, S.E., Hubbard, T. and Chothia, C. (1995) SCOP: a structural classification of proteins database for the investigation of sequences and structures. J. Mol. Biol. 247, 536–540.

[54] Garrett, R.M., Bellissimo, D.B. and Rajagopalan, K.V. (1995) Molecular cloning of human liver sulfite oxidase. Biochim. Biophys. Acta 1262, 147–149.

[55] Garrett, R.M. and Rajagopalan, K.V. (1994) Molecular cloning of rat-liver sulfite oxidase – expression of a eukaryotic Mo-pterin-containing enzyme in *Escherichia coli*. J. Biol. Chem. 269, 272–276.

[56] Barber, M.J. and Neame, P.J. (1990) A conserved cysteine in molybdenum oxotransferases. J. Biol. Chem. 265, 20912–20915.

[57] Toghrol, F. and Southerland, W.M. (1983) Purification of *Thiobacillus novellus* sulfite oxidase – evidence for the presence of heme and molybdenum. J. Biol. Chem. 258, 6762–6766.

[58] Johnson, J.L. and Rajagopalan, K.V. (1977) Tryptic cleavage of rat liver sulfite oxidase – isolation and characterization of molybdenum and heme domains. J. Biol. Chem. 252, 2017–2025.

[59] Nicholas, D.J.D. and A.J. Nason (1954) Molybdenum and nitrate reductase. II. Molybdenum as a constituent of nitrate reductase. J. Biol. Chem. 207, 353–360.

[60] Solomonson, L., Lorimer, G., Hall, R., Borchers, R. and Bailey, J. (1975) Reduced nicotinamide adenine dinucleotide nitrate reductase of *Chlorella vulgaris*. J. Biol. Chem. 250, 4120.

[61] Notton, B.A., Graf, L., Hewitt, E.J. and Povey, R.C. (1974) The role of molybdenum in the synthesis of nitrate reductase in cauliflower (*Brassica oleracea*) and spinach (*Spinacea oleracea*) Biochim. Biophys. Acta 364, 45–58.

[62] Kubo, Y., Ogura, N. and Nakagawa, H. (1988) Limited proteolysis of the nitrate reductase from spinach leaves. J. Biol. Chem. 263, 19684–19689.

[63] Lu, G., Lindqvist, Y., Schneider, G., Dwivedi, U. and Campbell, W.H. (1995) Structural studies on corn nitrate reductase – refined structure of the cytochrome *b* reductase fragment at 2.5 Å, its ADP complex and an active-site mutant and modeling of the cytochrome *b* domain. J. Mol. Biol. 248, 931–948.

[64] George, G.N., Kipke, C.A., Prince, R.C., Sunde, R.A., Enemark, J.H. and Cramer, S.P. (1989) Structure of the active site of sulfite oxidase. X-ray absorption spectroscopy of the Mo(IV), Mo(V), and Mo(VI) oxidation states. Biochemistry 28, 5075–5080.

[65] Rosner, B. and Schink, B. (1995) Purification and characterization of acetylene hydratase of *Pelobacter acetylenicus*, a tungsten iron–sulfur protein. J. Bacteriol. 177, 5767–5772.

[66] Kletzin, A. and Adams, M.W.W. (1996) Tungsten in biological systems. FEMS Microbiol. Rev. 18, 5–63.

[67] Zehnder, A.J.B. and Wuhrmann, K. (1976) Titanium (III)-citrate as a nontoxic oxidation-reduction buffering system for the culture of obligate anaerobes. Science 194, 1165–1166.

[68] Gladyshev, V.N., Boyington, J.C., Khangulov, S.V., Grahame, D.A., Stadtman, T.C. and Sun, P.D. (1996) Characterization of crystalline formate dehydrogenase_H from *Escherichia coli*. J. Biol. Chem. 271, 8095–8100.

[69] Cammack, R., Patil, D.S. and Fernandez, V.M. (1985) Electron-spin-resonance spectroscopy of iron–sulfur enzymes. Biochem. Soc. Trans. 13, 1463–1469.

[70] Yadav, J., Das, S.K. and Sarkar, S. (1997) A functional mimic of the new class of tungstoenzyme, acetylene hydratase. J. Am. Chem. Soc. 119, 4315–4316.

[71] Gibson, J., Dispensa, M., Harwood, C.S. (1997) 4-Hydroxybenzoyl coenzyme A reductase (dehydroxylating) is required for anaerobic degradation of 4-hydroxybenzoate by *Rhodopseudomonas palustris* and shares features with molybdenum-hydroxylases. J. Bacteriol. 179, 634–642.

[72] Breese, K. and Fuchs, G. (1997) 4-hydroxybenzoyl-CoA reductase (dehydroxylating) from the denitrifying bacterium *Thauera aromatica*. Prosthetic groups, electron donor, and genes of a member of the molybdenum–flavin–iron–sulfur proteins. Eur. J. Biochem. 251, 916–923.

[73] Canne, C., Stephan, I., Finsterbusch, J., Lingens, F., Kappl, R., Fetzner, S. and Hüttermann, J. (1997) Comparative EPR and redox studies of three prokaryotic enzymes of the xanthine oxidase family: quinoline 2-oxidoreductase, quinaldine 4-oxidase, and isoquinoline 1-oxidoreductase. Biochemistry 36, 9780–9790.